

Effective field theories and spin-wave excitations in helical magnets

Alexander I. Milstein*

Budker Institute of Nuclear Physics, 630090 Novosibirsk, Russia

Oleg P. Sushkov†

School of Physics, University of New South Wales, Sydney 2052, Australia

(Dated: January 14, 2013)

We consider two classes of helical magnets. The first one has magnetic ordering close to antiferromagnet and the second one has magnetic ordering close to ferromagnet. The first case is relevant to cuprate superconductors and the second case is realized in FeSrO_3 and FeCaO_3 . We derive the effective field theories for these cases and calculate corresponding excitation spectra. We demonstrate that the “hourglass” spin-wave dispersion observed experimentally in cuprates is a fingerprint of the “antiferromagnetic spin spiral state”. We also show that quantum fluctuations are important for the “ferromagnetic spin spiral”, they influence qualitative features of the spin-wave dispersion.

PACS numbers: 75.10.Jm, 74.72.Gh, 75.50.Ee, 75.50.Dd

I. INTRODUCTION

Helical spin systems have been studied for long time. Physics of these systems is fascinating and sometimes is very much different from that of collinear spin systems. The noncollinear spin systems manifest quite unusual temperature-driven phase transitions and critical properties,^{1–4} for a review see Ref. 5. Excitation spectra (magnons) in noncollinear systems are also very different from that in collinear magnets, see, e.g., Ref. 6. Generically there are two ways to generate a noncollinear spin structure, spin frustration and Dzyaloshinsky-Moriya spin orbit interaction. In the present paper we consider only the spin-frustration mechanism. It is worth to note that the Dzyaloshinsky-Moriya mechanism leads to interesting quantum field theories,^{7,8} but this is outside of the scope of the present work.

The usual field theory approach to a spin helix induced by spin frustration is based on the following representation of the spin \vec{S} , see Ref. 5

$$\vec{S}(t, \mathbf{r}) = \vec{a}(t, \mathbf{r}) \cos(\mathbf{Q} \cdot \mathbf{r}) + \vec{b}(t, \mathbf{r}) \sin(\mathbf{Q} \cdot \mathbf{r}). \quad (1)$$

Here \mathbf{Q} is the wave vector of the spin spiral and $\vec{a}(t, \mathbf{r})$, $\vec{b}(t, \mathbf{r})$ are the dynamic fields. The nonlinear Ginzburg-Landau action describing temperature-induced phase transitions is written in terms of the fields \vec{a} and \vec{b} , see review.⁵ Typically a frustration implies that $Q \sim 2\pi/a$, where a is the lattice spacing. Typical momenta, that appear in fluctuations of the \vec{a} and \vec{b} fields, are much smaller than Q , and hence \mathbf{Q} is not influenced by the fluctuations.

Sometimes, due to accidental fine tuning of parameters, the wave vector of the spin spiral is small, $Q \ll 2\pi/a$, i.e. the system is close to a collinear ferromagnet. This happens in FeSrO_3 and FeCaO_3 compounds.⁹ In this case typical momenta of fluctuations are comparable with Q , and hence the standard approach⁵ based on the Ginzburg-Landau action for \vec{a} and \vec{b} is not valid. Another example is the case of \mathbf{Q} close to the vector

of antiferromagnetic ordering. On the two-dimensional (2D) square lattice this means $\mathbf{Q} \rightarrow (\pi, \pi) + \mathbf{Q}$. This is the “antiferromagnetic spin spiral” realised in cuprate superconductors.^{10,11} In this case \mathbf{Q} is small because of the small doping x , and hence, once more, the approach based on Eq.(1) is not applicable.

There is one more important difference of the field theories considered in the present paper from the case (1). This difference concerns a direction of \mathbf{Q} . In the cases we consider, the vector \mathbf{Q} , in spite of being small, is always correlated with lattice directions. For example for a square lattice it can be directed only along a diagonal or along a side of the square. This implies an essential correlation between the short range dynamics, $\Delta x \sim a$, and the long range dynamics, $\Delta x \sim 1/Q$. Hence, this also implies that $O(3)$ and $SO(3)$ nonlinear σ -models cannot be applied for these situations.

In the present paper we consider effective quantum field theories for helical spin magnets close to antiferromagnets and to ferromagnets. The structure of the paper is the following. Section II reminds the reader the logic of derivations of the effective action for collinear antiferromagnets and ferromagnets. In Section III we consider the “antiferromagnetic spin spiral” and demonstrate that the “hourglass” spin-wave dispersion observed in neutron scattering from cuprates is a fingerprint of such state. In Section IV we consider the “ferromagnetic spin spiral” and show that quantum fluctuations influence qualitative features of the spin-wave dispersion. Section V presents our conclusions.

II. COLLINEAR ANTIFERROMAGNETS AND FERROMAGNETS

To derive the effective action for a collinear isotropic antiferromagnet (AF) one can use the following heuristic

tic arguments.¹ (i) The staggered magnetization is described by a unit vector \vec{n} , $\vec{n}^2 = 1$. (ii) The elastic energy is proportional to $(\nabla\vec{n})^2$. (iii) The Larmor theorem: If there is a state of the system without magnetic field, then the same state in a uniform magnetic field \vec{B} must precess with frequency $\omega = B$.² (iv) The static energy can depend on the magnetic field only quadratically because the system has no net magnetization. In other words, \vec{n} is not a vector, it is an axis. The only Lagrangian that satisfies the above requirements is the Lagrangian of the nonlinear σ -model

$$\mathcal{L}_{AF} = \frac{\chi_{\perp}}{2} \left(\dot{\vec{n}} - [\vec{n} \times \vec{B}] \right)^2 - \frac{\rho_s}{2} (\nabla\vec{n})^2, \quad (2)$$

where the coefficients are the perpendicular magnetic susceptibility χ_{\perp} and the spin stiffness ρ_s .

To derive the effective action for a collinear *ferromagnet* one can use similar arguments. (i) The magnetization is described by a unit vector \vec{n} , $\vec{n}^2 = 1$. (ii) The elastic energy is proportional to $(\nabla\vec{n})^2$. (iii) The Larmor theorem: If there is a state of the system without magnetic field, then the same state in a uniform magnetic field \vec{B} must precess with frequency $\omega = B$. (iv) The static energy depends on the magnetic field linearly because \vec{n} is true magnetization. The only Lagrangian that satisfies the above requirements reads

$$\begin{aligned} \mathcal{L}_F &= iS(\eta^\dagger \dot{\eta} - \dot{\eta}^\dagger \eta) - \frac{\rho_{\xi}}{2} (\nabla\vec{\xi})^2 + S(\vec{B} \cdot \vec{\xi}) \\ \vec{\xi} &= \eta^\dagger \vec{\sigma} \eta. \end{aligned} \quad (3)$$

Here S is spin of the ferromagnet and η is a CP^1 two-component spinor. The field $\vec{\xi}$ is a bosonic field, we just use the CP^1 representation for the field. Note that the difference between antiferro and ferro is only in the point (iv): quadratic or linear dependence of energy on an external uniform magnetic field.

It is worth reminding that Lagrangians and fields in a quantum field theory always depend on normalization point. Throughout the paper we use normalization at zero momentum (infinite distance). This implies that in the ground state the normalization is $|\langle\vec{n}\rangle| = |\langle\vec{\xi}\rangle| = 1$. This also implies that spin stiffnesses and the magnetic susceptibility in (2) and (3) are renormalized parameters that include all quantum fluctuations. These are not bare parameters.

In subsequent sections we derive and analyse effective actions that describe spin spiral states close to antiferromagnetic and ferromagnetic cases. This means that the wave vector of the corresponding spiral is small compared to the inverse lattice spacing. Specifically we have in mind cuprates for the AF case and FeCaO₃ for the ferro case.

III. SPIN SPIRAL CLOSE TO ANTIFERROMAGNET. BOSONIC FIELD THEORY INSPIRED BY CUPRATES

A. Effective action

Here we consider the 2D case (2D + time), the 3D generalization is straightforward. The effective action for the spin spiral state in the generalized $t - J$ model has been derived in Ref. 11. The action is written in terms of the bosonic field \vec{n} , describing staggered spins of the parent Mott insulator, and the fermionic field ψ_{α} describing mobile holons. The spinor ψ_{α} describes pseudospin of the holon, the pseudospin originates from two AF sublattices. The index $\alpha = a, b$ (flavor) describes a nodal pocket where the holon is located. The action reads

$$\begin{aligned} \mathcal{L} &= \frac{\chi_{\perp}}{2} \left(\dot{\vec{n}} - [\vec{n} \times \vec{B}] \right)^2 - \frac{\rho_s}{2} (\nabla\vec{n})^2 \\ &+ \sum_{\alpha} \left\{ \frac{i}{2} \left[\psi_{\alpha}^{\dagger} D_t \psi_{\alpha} - (D_t \psi_{\alpha})^{\dagger} \psi_{\alpha} \right] \right. \\ &+ \frac{\beta}{2} \psi_{\alpha}^{\dagger} \mathbf{D}^2 \psi_{\alpha} + \sqrt{2} g (\psi_{\alpha}^{\dagger} \vec{\sigma} \psi_{\alpha}) \cdot [\vec{n} \times (\mathbf{e}_{\alpha} \cdot \nabla) \vec{n}] \\ &\left. + \frac{1}{2} (\vec{B} \cdot \vec{n}) \psi_{\alpha}^{\dagger} (\vec{\sigma} \cdot \vec{n}) \psi_{\alpha} \right\}. \end{aligned} \quad (4)$$

The first line in the Lagrangian corresponds to the nonlinear σ -model (2) describing spins. The second line represents time derivatives of fermionic fields. The first term in the third line is the kinetic energy of fermions, β is the inverse mass, the second term in the third line was derived long time ago by Shraiman and Siggia.¹⁰ The last line represents the interaction of the pseudospin $\vec{\sigma}$ with an external uniform magnetic field.¹² The unit vectors $\mathbf{e}_a = (1/\sqrt{2}, 1/\sqrt{2})$ and $\mathbf{e}_b = (1/\sqrt{2}, -1/\sqrt{2})$ are directed along the corresponding diagonal of the square lattice. The original t - J model is gauge invariant. Therefore the effective action (4) is also gauge invariant and this is reflected in covariant derivatives

$$\begin{aligned} D_t &= \partial_t + \frac{i}{2} \vec{\sigma} \cdot [\vec{n} \times \dot{\vec{n}}] \\ \mathbf{D} &= \nabla + \frac{i}{2} \vec{\sigma} \cdot [\vec{n} \times \nabla\vec{n}], \end{aligned} \quad (5)$$

acting on the fermionic field.

The Lagrangian (4) describes many physical effects: superconductivity, spin spiral, particle-hole decay, even phase separation for some values of parameters. In the present work we aim only at the spin spiral. Therefore we will truncate fermionic degrees of freedom in (4) throwing away all physical effects except of the spin spiral. We retain only spin and pseudospin degrees of freedom responsible for the spin spiral. The way of truncation is pretty straightforward, we replace the fermionic field ψ_{α} by a bosonic field ξ_{α} describing pseudospin in the CP^1 representation

$$\psi_{\alpha}^{\dagger} \vec{\sigma} \psi_{\alpha} \rightarrow \xi_{\alpha}^{\dagger} = \eta_{\alpha}^{\dagger} \vec{\sigma} \eta_{\alpha}. \quad (6)$$

¹ A collinear state implies that the minimum dimensionality of the system is 2D + time.

² Hereafter we set $g\mu_B = 1$, g is the g-factor, and μ_B is Bohr magneton.

Hence, the truncated Lagrangian reads

$$\begin{aligned}\mathcal{L}_{AFS} = & \frac{\chi_{\perp}}{2} \left(\dot{\vec{n}} - [\vec{n} \times \vec{B}] \right)^2 - \frac{\rho_s}{2} (\nabla \vec{n})^2 \\ & + S_{\xi} \sum_{\alpha} \left\{ \frac{i}{2} \left(\eta_{\alpha}^{\dagger} D_t \eta_{\alpha} - (D_t \eta_{\alpha})^{\dagger} \eta_{\alpha} \right) \right. \\ & - \frac{\rho_{\xi}}{2} \left(\hat{D} \vec{\xi}_{\alpha} \right)^2 + \frac{g}{\sqrt{2}} \left(\vec{\xi}_{\alpha} \cdot [\vec{n} \times (\mathbf{e}_{\alpha} \cdot \nabla) \vec{n}] \right) \\ & \left. + \frac{1}{2} (\vec{B} \cdot \vec{n}) (\vec{\xi}_{\alpha} \cdot \vec{n}) \right\},\end{aligned}\quad (7)$$

where S_{ξ} is the effective “spin” of the ξ -field, the stiffness of the ξ -field is ρ_{ξ} . The coupling constant between \vec{n} and $\vec{\xi}$ fields is g , it does not coincide with g in (4), but they are related. Importantly, the truncated Lagrangian (7) still respects the gauge invariance of the original t-J model since it contains only covariant derivatives acting on the pseudospin, D_t is defined in Eq.(5), and the spacial derivative is defined as

$$\hat{D} \vec{\xi}_{\alpha} = \nabla \vec{\xi}_{\alpha} + \vec{\xi}_{\alpha} \times [\vec{n} \times \nabla \vec{n}]. \quad (8)$$

A related important point is that (7) respects also the Larmor theorem. If there is a state without magnetic field that satisfies equations of motion, then in a magnetic field this state precesses with frequency $\omega = B$. This is a sort of a global Ward identity.

It is worth noting that statuses of the Lagrangians (4) and (7) are different. The Lagrangian (4) has been derived from the generalized t-J model in a controlled way¹¹. The small parameter that controls accuracy of the derivation is small doping. On the other hand we obtain the Lagrangian (7) from (4) by an uncontrolled truncation of fermionic degrees of freedom. As a result we get an effective Ginzburg-Landau action (7) that contains only spin \vec{n} and pseudospin $\vec{\xi}$. In the present paper we analyze only the action (7) which, as we show below, describes experimental observations remarkably well.

The conventional approach⁵ to the spin spiral state is based on Eq. (1), it contains two vector dynamic fields $\vec{a}(t, \mathbf{r})$ and $\vec{b}(t, \mathbf{r})$. Our approach also contains two vector dynamic fields $\vec{n}(t, \mathbf{r})$ and $\vec{\xi}(t, \mathbf{r})$. The difference is that our effective action (7) is valid for any $q \ll 1$, it is not restricted by the region $q \ll Q$. We will show that in the limit $q \ll Q$ our approach results in two independent Goldstone modes with linear dispersions. Hence, as one should expect, in this limit both approaches are equivalent.

Hereafter we set the external magnetic field equal to zero, $B = 0$. Neglecting quantum fluctuations one can easily find the ground state of the Lagrangian (7),

$$\begin{aligned}\vec{n} &= (C, S, 0) \\ C &= \cos(\mathbf{Q} \cdot \mathbf{r}) \\ S &= \sin(\mathbf{Q} \cdot \mathbf{r}) \\ \vec{\xi}_a &= \vec{\xi}_b = (0, 0, 1) \\ \mathbf{Q} &= \frac{g}{\rho_s} \frac{\mathbf{e}_a + \mathbf{e}_b}{\sqrt{2}} = \frac{g}{\rho_s} (1, 0).\end{aligned}\quad (9)$$

Here we choose x- and y-directions in the spin space to lie in the plane of the spin spiral. Both $\vec{\xi}_a$ and $\vec{\xi}_b$ are directed along z in the spin space, and in this case the wave vector of the spiral \mathbf{Q} is directed along the (1,0) direction of the square lattice. One can also choose $\vec{\xi}_a = -\vec{\xi}_b = (0, 0, 1)$. In this case $\mathbf{Q} \propto \mathbf{e}_a - \mathbf{e}_b$ is directed along the (0,1) direction of the square lattice. The choice between these two possibilities is spontaneous.

B. The in-plane spin-wave excitation

Consider the spin-wave excitations above the ground state (9). There is the in-plane excitation $\varphi = \varphi(t, \mathbf{r})$, where

$$\begin{aligned}\vec{n} &= (\cos(\mathbf{Q} \cdot \mathbf{r} + \varphi), \sin(\mathbf{Q} \cdot \mathbf{r} + \varphi), 0) \\ \vec{\xi}_{\alpha} &= (0, 0, 1),\end{aligned}\quad (10)$$

and the out-of-plane excitation n_z , $\vec{\xi}_{\perp}$, where

$$\begin{aligned}\vec{n} &= (C, S, 0) \sqrt{1 - n_z^2} + (0, 0, n_z) \\ \vec{\xi}_{\alpha} &= (\xi_{\alpha x}, \xi_{\alpha y}, \sqrt{1 - \xi_{\alpha \perp}^2}) \\ \vec{\xi}_{\alpha \perp} &= (\xi_{\alpha x}, \xi_{\alpha y}, 0).\end{aligned}\quad (11)$$

Note that we use indexes x, y, z to denote axes in the spin space and we use indexes 1,2 to denote directions in the coordinate space, the direction 1 is parallel to the spin spiral vector \mathbf{Q} and the direction 2 is perpendicular to the spin spiral vector.

We first consider the in-plane magnon (10) that does not involve fluctuations of the ξ -field. Substituting expression (10) in the Lagrangian (7) and keeping only quadratic terms in the small perturbation φ one finds

$$\mathcal{L} \rightarrow \frac{\chi_{\perp}}{2} \dot{\varphi}^2 - \frac{\rho_s}{2} (\nabla \varphi)^2. \quad (12)$$

Hence the Green's function of the in-plane magnon is the same as the Green's function of a magnon in the parent σ -model,

$$G_{\varphi}(\omega, \mathbf{q}) = \frac{\chi_{\perp}^{-1}}{\omega^2 - c^2 q^2 + i0}, \quad (13)$$

where

$$c = \sqrt{\frac{\rho_s}{\chi_{\perp}}} \quad (14)$$

is the bare spin-wave speed. The in-plane magnons can be excited in inelastic neutron scattering. Neutrons interact only with the n -field that represents real spins, therefore the scattering amplitude is given by the Fourier transform of \vec{n} from (10) and the scattering probability for unpolarized neutrons with the energy transfer ω and the momentum transfer \mathbf{k} is proportional to

$$I_{in}(\omega, \mathbf{k}) = -\frac{1}{2\pi} \text{Im} [G_{\varphi}(\omega, \mathbf{k} - \mathbf{Q}) + G_{\varphi}(\omega, \mathbf{k} + \mathbf{Q})] \quad (15)$$

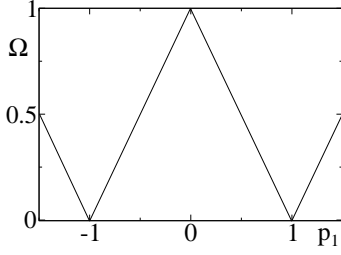


FIG. 1: The spin wave dispersion of the in-plane magnon as it is seen in neutron scattering

Hereafter we introduce the dimensionless energy and the dimensionless momentum

$$\Omega = \frac{\omega}{cQ}, \quad \mathbf{p} = \frac{\mathbf{q}}{Q}. \quad (16)$$

The momentum is measured in units of the wave vector of the spin spiral and the energy is measured in units of the magnon energy in the parent σ -model with momentum of the magnon equal to the spin spiral wave vector. According to Eq.(15) the in-plane magnon is seen in neutron scattering as two cones originating from the points $\pm \mathbf{Q}$. The corresponding plot for the direction along the spin spiral is shown in Fig. 1.

C. The out-of-plane spin-wave excitation

We have shown in the previous subsection that the in-plane magnon in the spin-spiral state remains trivial. It is not the case for the out-of-plane magnon. Substitution of (11) in Eq.(7) gives the following action expressed in terms of n_z and $\xi_{\alpha\perp}$

$$\begin{aligned} \mathcal{L}_{AFS} = & \frac{\chi_{\perp}}{2} \dot{n}_z^2 - \frac{\rho_s}{2} [Q^2(1 - n_z^2) + (\nabla n_z)^2] \quad (17) \\ & + S_{\xi} \sum_{\alpha} \left\{ \frac{i}{2} (\eta_{\alpha}^{\dagger} \dot{\eta}_{\alpha} - \dot{\eta}_{\alpha}^{\dagger} \eta_{\alpha}) - \frac{1}{2} (S\xi_{\alpha x} - C\xi_{\alpha y}) \dot{n}_z \right\} \\ & - \frac{\rho_{\xi}}{2} \sum_{\alpha} \left[(\nabla \xi_{\alpha x} + \mathbf{Q} \xi_{\alpha y} + S \mathbf{Q} n_z + C \nabla n_z)^2 \right. \\ & + (\nabla \xi_{\alpha y} - \mathbf{Q} \xi_{\alpha x} - C \mathbf{Q} n_z + S \nabla n_z)^2 \left. \right] \\ & + \frac{g}{\sqrt{2}} \sum_{\alpha} \mathbf{e}_{\alpha} \left[\mathbf{Q} \left(1 - n_z^2 - \frac{1}{2} \xi_{\alpha\perp}^2 \right) \right. \\ & + (-C\xi_{\alpha x} - S\xi_{\alpha y}) \mathbf{Q} n_z + (S\xi_{\alpha x} - C\xi_{\alpha y}) \nabla n_z \left. \right]. \end{aligned}$$

We keep here only quadratic terms. Let us perform in (17) two subsequent gauge transformations. The first one is

$$\begin{aligned} \eta_{\alpha} &= \exp \left\{ -\frac{i}{2} (\mathbf{Q} \cdot \mathbf{r}) \sigma_z \right\} \eta'_{\alpha} \\ \xi_{\alpha x} &= C\xi'_{\alpha x} - S\xi'_{\alpha y} \\ \xi_{\alpha y} &= S\xi'_{\alpha x} + C\xi'_{\alpha y}. \end{aligned} \quad (18)$$

The second transformation reads

$$\begin{aligned} \eta'_{\alpha} &= \exp \left\{ \frac{i}{2} n_z \sigma_y \right\} \eta''_{\alpha} \\ \xi'_{\alpha x} &\approx \xi''_{\alpha x} - n_z \\ \xi'_{\alpha y} &= \xi''_{\alpha y}. \end{aligned} \quad (19)$$

Geometrically the gauge transformations (18) and (19) describe the transition to the proper reference frame of the vibrating spin spiral. In terms of the new variables η'' and ξ'' the Lagrangian (17) consists of three parts

$$\begin{aligned} \mathcal{L}_{AFS} &= \mathcal{L}_n + \mathcal{L}_{\xi} + \mathcal{L}_{int} \quad (20) \\ \mathcal{L}_n &= \frac{\chi_{\perp}}{2} \dot{n}_z^2 - \frac{\rho_s}{2} (\nabla n_z)^2 - \rho_{\xi} Q^2 n_z^2 \\ \mathcal{L}_{\xi} &= \sum_{\alpha} \left\{ S_{\xi} \frac{i}{2} (\eta_{\alpha}^{\dagger} \dot{\eta}_{\alpha} - \dot{\eta}_{\alpha}^{\dagger} \eta_{\alpha}) \right. \\ &\quad \left. - \frac{\rho_{\xi}}{2} [(\nabla \xi_{\alpha x})^2 + (\nabla \xi_{\alpha y})^2] - \rho_s \frac{Q^2}{4} \xi_{\alpha\perp}^2 \right\} \\ \mathcal{L}_{int} &= \sum_{\alpha} \left\{ -\frac{g}{\sqrt{2}} \xi_{\alpha y} (\mathbf{e}_{\alpha} \cdot \nabla) n_z + \rho_{\xi} n_z (\mathbf{Q} \cdot \nabla) \xi_{\alpha y} \right\}. \end{aligned}$$

Hereafter we skip the double prime in notations of η'' and ξ'' . The first part, \mathcal{L}_n , describes the free motion of the n_z -field; the second part, \mathcal{L}_{ξ} , describes the free motion of the ξ -fields; and the third part, \mathcal{L}_{int} , describes the interaction between n_z and ξ . Equations of motion generated by the action (20) are

$$\begin{aligned} \chi_{\perp} \ddot{n}_x &= \rho_s \Delta n_z - 2\rho_{\xi} Q^2 n_z \\ &\quad + \sum_{\alpha} \left[\frac{g}{\sqrt{2}} (\mathbf{e}_{\alpha} \cdot \nabla) \xi_{\alpha y} + \rho_{\xi} (\mathbf{Q} \cdot \nabla) \xi_{\alpha y} \right] \\ S_{\xi} \dot{\xi}_{\alpha x} &= -2 \left[\rho_{\xi} \Delta \xi_{\alpha y} - \frac{\rho_s Q^2}{2} \xi_{\alpha y} \right. \\ &\quad \left. - \frac{g}{\sqrt{2}} (\mathbf{e}_{\alpha} \cdot \nabla) n_z - \rho_{\xi} (\mathbf{Q} \cdot \nabla) n_z \right] \\ S_{\xi} \dot{\xi}_{\alpha y} &= 2 \left[\rho_{\xi} \Delta \xi_{\alpha x} - \frac{\rho_s Q^2}{2} \xi_{\alpha x} \right]. \end{aligned} \quad (21)$$

Looking for solution in the form

$$\begin{aligned} n_z &= A e^{-i\omega t + i\mathbf{q} \cdot \mathbf{r}} \\ \xi_{\alpha x} &= B_{\alpha} e^{-i\omega t + i\mathbf{q} \cdot \mathbf{r}} \\ \xi_{\alpha y} &= -iC_{\alpha} e^{-i\omega t + i\mathbf{q} \cdot \mathbf{r}} \end{aligned} \quad (22)$$

we find the relations between the coefficients A , B_{α} , C_{α} , and the frequencies of excitations,

$$\begin{aligned} \Omega_{1,p}^2, \Omega_{2,p}^2 &= \frac{1}{2} (O_1 + O_2) \mp \sqrt{\frac{1}{4} (O_1 - O_2)^2 + O_3} \\ O_1 &= p^2 + b^2 \\ O_2 &= a^2 (1 + b^2 p^2)^2 \\ O_3 &= a^2 (1 + b^2 p^2) [p_1^2 (1 + b^2)^2 + p_2^2] \\ p^2 &= p_1^2 + p_2^2. \end{aligned} \quad (23)$$

These equations are written in terms of dimensionless frequency and momentum (16). We remind that p_1 is parallel to \mathbf{Q} and p_2 is perpendicular to \mathbf{Q} . In (23) we have introduced two dimensionless parameters

$$a = \frac{Q\rho_s}{cS\xi}, \quad b = \sqrt{\frac{2\rho_\xi}{\rho_s}}. \quad (24)$$

Note that these parameters are unrelated to the a,b-flavors.

Importantly, there are two branches of the dispersion that originate from two different degrees of freedom, spin \vec{n} and pseudospin $\vec{\xi}$. In order to reproduce the spin-wave excitation spectra of the t-J model at small doping we chose $b \ll 1$, $a > b$. The parameter b defined in (24) determines the top of the lower branch $\Omega_{1,\mathbf{p}}$, and the parameter a defined in (24) determines the bottom of the upper branch $\Omega_{2,\mathbf{p}}$. Plots of $\Omega_{1,\mathbf{p}}$ and $\Omega_{2,\mathbf{p}}$, for directions of \mathbf{p} parallel to the spin spiral and perpendicular to the spin spiral are presented in Figs. 2A,B for values of parameters $b = 0.25$, $a = 0.5$. Similar plots for $b = 0.25$, $a = 0.3$ are presented in Figs. 3A,B. In Figs. 2 and 3 the

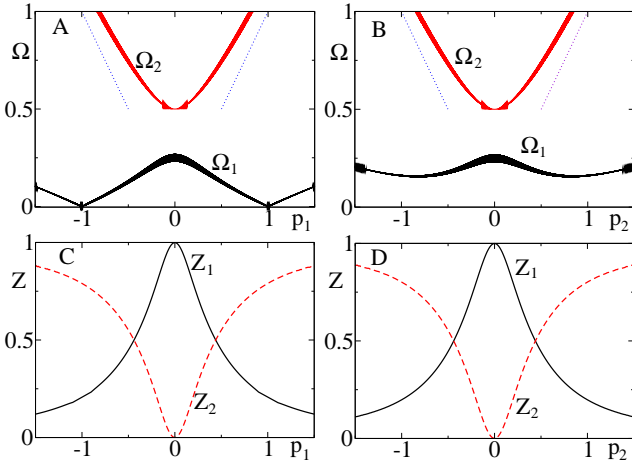


FIG. 2: (Color online) A and B: the dispersion $\Omega_{\mathbf{k}}$ of the out-of-plane magnon in directions parallel to the spin spiral, (A); and perpendicular to the spin spiral, (B). Values of parameters of the effective field theory are $a = 0.5$, $b = 0.25$. The blue dotted lines show the magnon dispersion in the parent σ -model. Thickness of Ω_1 and Ω_2 lines is proportional to the corresponding quasiparticle residue Z_1 , Z_2 . The quasiparticle residues are plotted separately for the same directions in Figs. C and D.

dispersion is shown by very thick lines. The thickness is not a decay width, the decay width in this approximation (no alive fermions) is negligible. The thickness is proportional to the corresponding quasiparticle residue calculated below.

To find absolute values of the coefficients A , B_α , C_α , in (22) we need to quantize (20). There are two magnon creation operators, $c_{1,\mathbf{p}}^\dagger$, and $c_{2,\mathbf{p}}^\dagger$, corresponding to two branches of the dispersion. The standard quantization

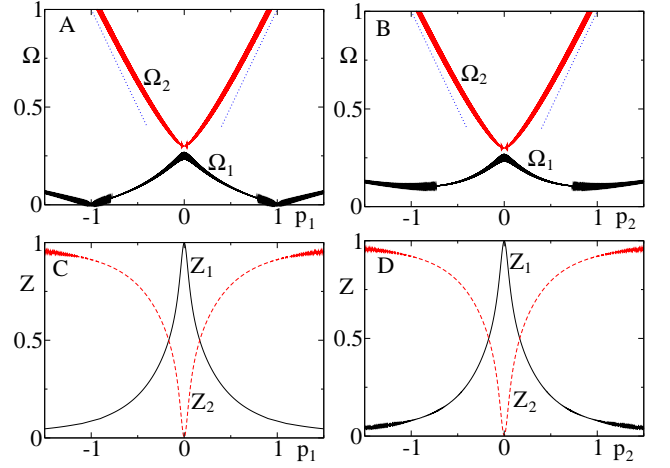


FIG. 3: (Color online) A and B: the dispersion $\Omega_{\mathbf{k}}$ of the out-of-plane magnon in directions (A) parallel to the spin spiral, and (B) perpendicular to the spin spiral. Values of parameters of the effective field theory are $a = 0.3$, $b = 0.25$. The blue dotted lines show the magnon dispersion in the parent σ -model. Thickness of Ω_1 and Ω_2 lines is proportional to the corresponding quasiparticle residue Z_1 , Z_2 . The quasiparticle residues are plotted separately for the same directions in Figs. C and D.

gives

$$n_z = \sum_{l=1,2} N_{l,\mathbf{p}} + h.c. \quad (25)$$

$$N_{l,\mathbf{p}} = \frac{1}{\sqrt{\chi_\perp cQ}} \sqrt{\frac{Z_{l,\mathbf{p}}}{2\Omega_{l,\mathbf{p}}}} c_{l\mathbf{p}} e^{-i\omega t + i\mathbf{q} \cdot \mathbf{r}}$$

$$\xi_{\alpha x} = - \sum_{l=1,2} \frac{a\Omega_{l,\mathbf{p}} [\sqrt{2}(e_\alpha \cdot \mathbf{p}) + b^2 p_1]}{\Omega_{l,\mathbf{p}}^2 - O_2} N_{l,\mathbf{p}} + h.c.$$

$$\xi_{\alpha y} = i \sum_{l=1,2} \frac{a^2(1 + b^2 p^2) [\sqrt{2}(e_\alpha \cdot \mathbf{p}) + b^2 p_1]}{\Omega_{l,\mathbf{p}}^2 - O_2} N_{l,\mathbf{p}} + h.c.$$

Here index $l = 1, 2$ enumerates the dispersion branches, the expression for O_2 is given in (23), and $Z_{l,\mathbf{p}}$ is the quasiparticle residue

$$Z_{1,\mathbf{p}}, Z_{2,\mathbf{p}} = \frac{1}{2} \left\{ 1 \mp \frac{(O_1 - O_2)}{\sqrt{(O_1 - O_2)^2 + 4O_3}} \right\}. \quad (26)$$

The quasiparticle residues $Z_{1,\mathbf{p}}$ and $Z_{2,\mathbf{p}}$ are plotted in Figs. 2 C,D and in Figs. 3 C,D. Interestingly, the quasiparticle residues are practically isotropic, the dependence on the direction of \mathbf{p} is extremely weak. The magnon Green's function defined in the standard way reads

$$\begin{aligned} G_{n_z}(\omega, \mathbf{q}) &= -i \int \langle T \{ n_z(\mathbf{r}, t) n_z(0, 0) \} \rangle e^{i\omega t - i\mathbf{q} \cdot \mathbf{r}} dt d^2 r \\ &= \frac{\chi_\perp^{-1} Z_{1,\mathbf{q}}}{\omega^2 - \omega_{1,\mathbf{q}}^2 + i0} + \frac{\chi_\perp^{-1} Z_{2,\mathbf{q}}}{\omega^2 - \omega_{2,\mathbf{q}}^2 + i0}. \end{aligned} \quad (27)$$

We remind that ω , Ω and \mathbf{q} , \mathbf{p} are related according to Eq.(16). The inelastic neutron scattering intensity for

unpolarized neutrons with the energy transfer ω and the momentum transfer \mathbf{k} is proportional to

$$I_{out}(\omega, \mathbf{k}) = -\frac{1}{\pi} \text{Im } G_{n_z}(\omega, \mathbf{k}) \quad (28)$$

Figs. 2 and 3 show the “hourglass” dispersion that agrees with the typical dispersion observed in cuprates.^{13–15} The lower branch $\Omega_{1,\mathbf{q}}$ has strongly anisotropic momentum dependence with zeros at the Goldstone points $\mathbf{q} = \pm\mathbf{Q}$, while the upper branch $\Omega_{2,\mathbf{q}}$ is practically isotropic in the momentum space quickly approaching the bare spin-wave dispersion at larger q . The intensity (quasiparticle residue) of the lower branch $Z_{1,\mathbf{q}}$ is strongly peaked at $\mathbf{q} = 0$, at the “neck” of the “hourglass”, and the intensity decays dramatically away from this point, see Figs. 2 C,D and Figs. 3 C,D. On the other hand the intensity of the upper branch $Z_{2,\mathbf{q}}$ is zero exactly at $\mathbf{q} = 0$ and quickly approaches unity away from this point. The dispersion obtained in the present work demonstrates that the “hourglass” shape is a “fingerprint” of the spin spiral driven by the interaction between spin and pseudospin. The two branches Ω_1 and Ω_2 reflect the two degrees of freedom: spin and pseudospin.

D. Quantum fluctuations

The spin spiral state that we consider can be characterized by the vector order parameters, that indicate ordering of spin \vec{n} and pseudospin $\vec{\xi}$, and a pseudoscalar order parameter \mathcal{P} that indicates chirality. The order parameters are

$$\begin{aligned} \langle \vec{n} \rangle, \quad \langle \vec{\xi}_a \rangle, \quad \langle \vec{\xi}_b \rangle \\ \mathcal{P} = \langle \frac{1}{\sqrt{2}} \sum_{\alpha} \vec{\xi}_{\alpha} \cdot [\vec{n} \times (\mathbf{e}_{\alpha} \cdot \nabla) \vec{n}] \rangle. \end{aligned} \quad (29)$$

In semiclassical approximation values of the vector order parameters are given by Eqs. (9), the chiral pseudoscalar is $\mathcal{P} = Q$. Note that \mathcal{P} changes sign under time reflection.

Due to quantum fluctuations values of some order parameters are reduced. The reduction of the spin field is

$$|\langle \vec{n} \rangle| = \langle \sqrt{1 - \varphi^2 - n_z^2} \rangle \approx 1 - \frac{1}{2} \langle \varphi^2 \rangle - \frac{1}{2} \langle n_z^2 \rangle. \quad (30)$$

Only the length is reduced, the spacial dependence is still given by Eq. (9), $\langle \vec{n} \rangle = |\langle n \rangle| (\cos(\mathbf{Q} \cdot \mathbf{r}), \sin(\mathbf{Q} \cdot \mathbf{r}), 0)$. To calculate the reduction of the length we note that the expectation values $\langle \varphi^2 \rangle$ and $\langle n_z^2 \rangle$ can be expressed in terms of the Green’s function,

$$\begin{aligned} \langle \varphi^2 \rangle &= - \sum_{\mathbf{q}} \int \frac{d\omega}{2\pi i} G_{in}(\omega, \mathbf{q}) \\ \langle n_z^2 \rangle &= - \sum_{\mathbf{q}} \int \frac{d\omega}{2\pi i} G_{out}(\omega, \mathbf{q}). \end{aligned} \quad (31)$$

The physical meaning of relations (30) and (31) is very simple: the reduction of static response is transferred to the dynamic response. The expressions (30) and (31) must be renormalized by subtraction of the ultraviolet-divergent contribution that corresponds to the parent σ -model. Since the Green’s function of the in-plane excitation (13) is exactly the same as the magnon Green’s function in the parent σ -model, the fluctuation $\langle \varphi^2 \rangle$ is renormalized to zero. The out-of plane fluctuation gives

$$\begin{aligned} |\langle \vec{n} \rangle| &\approx 1 - \frac{1}{2} \langle n_z^2 \rangle = 1 - \frac{cQ}{2\rho_s} \mathcal{I}_R \\ \mathcal{I}_R &= \int \left\{ \frac{Z_{1,\mathbf{p}}}{2\Omega_{1,\mathbf{p}}} + \frac{Z_{2,\mathbf{p}}}{2\Omega_{2,\mathbf{p}}} - \frac{1}{2p} \right\} \frac{d^2 p}{(2\pi)^2}. \end{aligned} \quad (32)$$

Here the subscript R stands for “renormalized”, $\mathcal{I} \rightarrow \mathcal{I}_R$. The dimensionless integral \mathcal{I}_R can be easily calculated, it depends only on the parameters b and a defined in (24). Values of the integral for a and b corresponding to Figs. 2,3 are

$$\begin{aligned} \mathcal{I}_R(a = 0.5, b = 0.25) &= 0.23 \\ \mathcal{I}_R(a = 0.3, b = 0.25) &= 0.15. \end{aligned} \quad (33)$$

The pseudospin $\vec{\xi}_{\alpha}$ is not a gauge invariant object, it cannot be directly measured and its expectation value depends on gauge. One can calculate the expectation value of $\vec{\xi}_{\alpha}$ defined in the original action (7) or one can calculate the expectation value of $\vec{\xi}_{\alpha}''$ obtained after the gauge transformation (18), (19). Below we calculate $\langle (\xi_{\alpha\perp}'')^2 \rangle$, but we skip the double prime in notations. Using Eqs. (25) we find

$$\begin{aligned} \langle \xi_{\alpha\perp}^2 \rangle &= \langle \xi_{\alpha x}^2 \rangle + \langle \xi_{\alpha y}^2 \rangle = \frac{cQ}{\rho_s} \mathcal{J} \\ \mathcal{J} &= \int \sum_{l=1,2} \frac{Z_{l,\mathbf{p}}}{2\Omega_{l,\mathbf{p}}} \frac{a^2 [\Omega_{l,\mathbf{p}}^2 + O_2] [p_1^2 (1+b^2)^2 + p_2^2]}{[\Omega_{l,\mathbf{p}}^2 - O_2]^2} \frac{d^2 p}{(2\pi)^2}. \end{aligned} \quad (34)$$

At $p \rightarrow \infty$ the integrand in \mathcal{J} is approaching the constant value equal to a . This corresponds to the ultraviolet divergence of $\langle \xi_{\alpha}^2 \rangle$ in the parent ξ -model defined by Eq. (3). Therefore \mathcal{J} must be renormalized, $\mathcal{J} \rightarrow \mathcal{J}_R$, in the following way

$$\mathcal{J}_R = \int \{(\dots) - a\} \frac{d^2 p}{(2\pi)^2}, \quad (35)$$

where (...) stands for the integrand in (34). After the renormalization \mathcal{J}_R is convergent.

The chiral pseudoscalar order parameter \mathcal{P} is defined in Eq. (29). In this definition the field ξ_{α} is the pseudospin of the original action (7), and in this sense the chiral order parameter is gauge invariant. It is easy to rewrite the order parameter in terms of the gauge transformed ξ_{α}'' and n_z ,

$$\frac{\mathcal{P}}{Q} = 1 - \frac{1}{2} \langle n_z^2 \rangle - \frac{1}{2} \langle \xi_{\alpha\perp}^2 \rangle - \frac{1}{\sqrt{2}Q} \langle \sum_{\alpha} \xi_{\alpha y} (\mathbf{e}_{\alpha} \cdot \nabla) n_z \rangle, \quad (36)$$

where we again omit the double prime in notations. The first two terms after the unity have been already calculated in Eqs.(32),(34), and the last term immediately follows from (25),

$$\frac{1}{\sqrt{2}Q} \langle \sum_{\alpha} e_{\alpha} \xi_{\alpha y} \nabla n_z \rangle = \frac{cQ}{2\rho_s} \mathcal{K} \quad (37)$$

$$\mathcal{K} = \int \sum_{l=1,2} \frac{Z_{l,\mathbf{p}}}{2\Omega_{l,\mathbf{p}}} \frac{2a^2[1+b^2p^2][p^2+b^2p_1^2]}{[\Omega_{l,\mathbf{p}}^2 - O_2]} \frac{d^2p}{(2\pi)^2}.$$

The integrand in \mathcal{K} decays at large p as $\propto 1/p$, so \mathcal{K} is ultraviolet divergent. We will discuss this divergence in subsection E.

Quantum fluctuations do not influence direction of the spin spiral wave vector \mathbf{Q} , but they change the absolute value of the vector. To calculate the quantum fluctuation correction to \mathbf{Q} we need to account for nonlinear terms in the Lagrangian (7). To do so it is convenient to generalize the notations (10) and (11) for the in-plane and out-of-plane excitations in the following way

$$\begin{aligned} \vec{n} &= (C_{\varphi}, S_{\varphi}, 0)C_{\gamma} + (0, 0, 1)S_{\gamma} \\ \vec{\xi}_{\alpha} &= (\xi_{\alpha x}, \xi_{\alpha y}, \sqrt{1 - \xi_{\alpha\perp}^2}) \\ C_{\varphi} &= \cos(\mathbf{Q} \cdot \mathbf{r} + \varphi) \\ S_{\varphi} &= \sin(\mathbf{Q} \cdot \mathbf{r} + \varphi) \\ C_{\gamma} &= \cos \gamma \\ S_{\gamma} &= n_z = \sin \gamma. \end{aligned} \quad (38)$$

The gauge transformation (18),(19) is generalized as

$$\begin{aligned} \eta_{\alpha} &= \exp \left\{ -\frac{i}{2} (\mathbf{Q} \cdot \mathbf{r} + \varphi) \sigma_z \right\} \exp \left\{ \frac{i}{2} \gamma \sigma_y \right\} \eta''_{\alpha} \\ \xi_{\alpha x} &= C_{\varphi} (C_{\gamma} \xi''_{\alpha x} - S_{\gamma} \xi''_{\alpha z}) - S_{\varphi} \xi''_{\alpha y} \\ \xi_{\alpha y} &= S_{\varphi} (C_{\gamma} \xi''_{\alpha x} - S_{\gamma} \xi''_{\alpha z}) + C_{\varphi} \xi''_{\alpha y} \\ \xi_{\alpha z} &= S_{\gamma} \xi''_{\alpha x} + C_{\gamma} \xi''_{\alpha z}. \end{aligned} \quad (39)$$

Substitution of this transformation in (7) gives the quadratic Lagrangian (20) as well as the following cubic term (again we omit the double prime in ξ)

$$\begin{aligned} \mathcal{L}_3 &= \rho_s \left\{ \left(\frac{1}{2} - b^2 \right) n_z^2 \mathbf{Q} - \frac{Q}{2\sqrt{2}} \sum_{\alpha} \xi_{\alpha\perp}^2 \mathbf{e}_{\alpha} \right. \\ &\quad \left. + \frac{b^2}{2} \sum_{\alpha} (\nabla \xi_{\alpha y}) n_z \right\} \nabla \varphi \end{aligned} \quad (40)$$

By calculating the tadpole with φ as an external leg, see Fig. 4, we find

$$\begin{aligned} \mathcal{L}_3 &\rightarrow \rho_s (\mathbf{Q} \cdot \nabla) \varphi \\ &\times \left\{ \left(\frac{1}{2} - b^2 \right) \langle n_z^2 \rangle - \frac{1}{2} \langle \xi_{\alpha\perp}^2 \rangle - \frac{b^2}{2Q^2} \langle \sum_{\alpha} \xi_{\alpha y} (\mathbf{Q} \cdot \nabla) n_z \rangle \right\} \end{aligned} \quad (41)$$

Value of the wave vector of the spin spiral follows from the condition that there are no linear in $\nabla \varphi$ terms in the

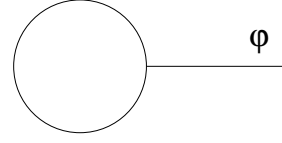


FIG. 4: The tadpole diagram giving the quantum correction to the spin spiral wave vector.

effective action. The corresponding term in (7) in the leading approximation is $-\rho_s (\mathbf{Q} \cdot \nabla) \varphi + \frac{Q}{\sqrt{2}} \sum_{\alpha} (\mathbf{e}_{\alpha} \cdot \nabla \varphi)$. The condition of the disappearance of this term gives the value of Q presented in Eq. (9). The account of the tadpole (41) gives the quantum correction to the spiral vector,

$$\begin{aligned} \frac{\delta Q}{Q} &= \left(\frac{1}{2} - b^2 \right) \langle n_z^2 \rangle - \frac{1}{2} \langle \xi_{\alpha\perp}^2 \rangle \\ &\quad - \frac{b^2}{2Q^2} \langle \sum_{\alpha} \xi_{\alpha y} (\mathbf{Q} \cdot \nabla) n_z \rangle. \end{aligned} \quad (42)$$

The last term here is very similar to (37),

$$\begin{aligned} \frac{1}{2Q^2} \langle \sum_{\alpha} \xi_{\alpha y} (\mathbf{Q} \cdot \nabla) n_z \rangle &= \frac{cQ}{2\rho_s} \mathcal{K}' \\ \mathcal{K}' &= \int \sum_{l=1,2} \frac{Z_{l,\mathbf{p}}}{2\Omega_{l,\mathbf{p}}} \frac{2a^2[1+b^2p^2][1+b^2]p_1^2}{[\Omega_{l,\mathbf{p}}^2 - O_2]} \frac{d^2p}{(2\pi)^2}. \end{aligned} \quad (43)$$

It is also ultraviolet divergent. We discuss the divergence in the next subsection.

E. Discussion and conclusion of the “antiferromagnetic spiral” section

Both \mathcal{K} in Eq.(37) and \mathcal{K}' in Eq.(43) are ultraviolet divergent. There is no a formal way to renormalize out these ultraviolet divergences. The effective bosonic field theory defined by the action (7) is unrenormalizable. Practically this means that quantum corrections depend on the ultraviolet cutoff and different physical quantities depend on this cutoff in different ways. So it is impossible to reduce renormalization of all physical quantities to the renormalization of a finite set of parameters.

Thus, the simplest conclusion is that within the effective low energy bosonic theory (7) one can calculate the spin-wave spectra. The results are presented in Figs. 1,2,3. On the other hand it is impossible to calculate quantum corrections. However, we can somewhat improve the situation if recall that the effective action (7) originates from the effective action (4) that is equivalent to the t-J model at low doping. Therefore, the ultraviolet cutoff for fluctuations of the n -field (32) is about the inverse lattice spacing, $\Lambda_n \sim 1/a$. This cutoff does not appear in our results explicitly as soon as we use the renormalized spin stiffness and spin-wave velocity of the Heisenberg model¹⁶ $\rho_s = 0.18J$, $c = 1.65J$ (we set the

lattice spacing equal to unity, $a = 1$). The ultraviolet cut-off for fluctuations of the ξ -field (34), (37), (43) is of the order of the Fermi momentum of holes, $\Lambda_\xi \sim p_F \sim \sqrt{\pi x}$, where $x \ll 1$ is the doping level. At $q > p_F$ description of fermions in terms of a structureless bosonic field ξ does not make sense. The wave vector of the spin spiral scales linearly with doping¹¹, $Q \propto x$. Therefore, we conclude from Eqs. (37) and (43) that the quantum fluctuation corrections to the spiral wave vector and to the pseudoscalar order parameter are

$$\frac{\delta Q}{Q} \propto b^2 \sqrt{x}, \quad \frac{\delta \mathcal{P}}{\mathcal{P}} \propto +\sqrt{x}. \quad (44)$$

The \sqrt{x} dependence originate from the integrals \mathcal{K} and \mathcal{K}' that are regularized by imposing the ultraviolet cut-off $\Lambda_\xi \sim \sqrt{x}$. There are two important points about Eqs.(44). (i) The quantum correction to the spiral wave vector is proportional to b^2 . According to experimental spectra¹³⁻¹⁵ $b \lesssim 0.25$ and hence $b^2 \lesssim 0.06$. So, we predict a very small quantum correction to the vector of the spin spiral. (ii) The sign of the $\delta \mathcal{P}$ is positive since \mathcal{K} in (37) is negative. Hence quantum fluctuations enhance the pseudoscalar order parameter. This trend is opposite to the trend in $\langle \vec{n} \rangle$. According to Eq. (32) quantum fluctuations reduce value of $|\langle \vec{n} \rangle|$ and at a sufficiently large Q the static component of spin vanishes, $|\langle \vec{n} \rangle| = 0$. Disappearance of static spin does not mean that the spin spiral disappears, the spin spiral just becomes dynamic. Hence, $|\langle \vec{n} \rangle| = 0$ indicates the Quantum Critical Point (QCP) for transition from the static spin spiral to the dynamic one. The spin spiral itself is characterised by the pseudoscalar chiral order parameter \mathcal{P} independently whether this is static or dynamic case. This order parameter goes smoothly through the QCP. So, the spin spiral survives in the magnetically disordered phase.

There are two types of spin wave excitations, the in-plane magnons and the out-of-plane magnons. The spectrum of the in-plane magnons is given by Eq.(15) and Fig. 1, and that of the out-of-plane magnons is given by Eq.(28) and Figs. 2,3. It follows from Eq.(15) that neutron scattering with excitation of in-plane magnons is necessarily accompanied by diffraction on the static spiral. Therefore, one should expect that the intensity of the inelastic neutron scattering with excitation of in-plane magnons is sharply decreasing at approaching the QCP. The intensity is zero in the magnetically disordered phase. On the other hand the intensity of neutron scattering with excitation of out-of-plane magnons (Figs. 2,3 with the hourglass dispersion) is not related to a diffraction and hence it is not very sensitive to the QCP. The two branches of the hourglass dispersion originate from two different degrees of freedom, spin and pseudospin. The lower branch of the hourglass has strongly anisotropic momentum dependence with zeros at the Goldstone points $\mathbf{q} = \pm \mathbf{Q}$, while the upper branch is practically isotropic. This behavior agrees with the typical dispersion observed in cuprates.¹³⁻¹⁵

IV. SPIN SPIRAL CLOSE TO FERROMAGNET. THE FIELD THEORY INSPIRED BY FeSrO₃

The present section is inspired by neutron scattering data⁹ from FeSrO₃ and FeCaO₃ that indicate the spin spiral close to a collinear ferromagnet. The wave length of the spin spiral in FeSrO₃ is about 10 lattice spacing. The compound is an insulator, therefore there is only a spin field in the game, there is no a pseudospin, and there is no other relevant dynamic variable. To understand the kinematic structure of the effective action we refer to the minimal Heisenberg model suggested in Ref.¹⁷ In the present paper we consider generic scenarios, therefore we address for simplicity the 2D case. The 3D generalization is straightforward.

A. Effective action

The Hamiltonian of the minimal Heisenberg model is

$$H = -J_1 \sum_{ij} \vec{S}_i \cdot \vec{S}_j + J_2 \sum_{i'j'} \vec{S}_{i'} \cdot \vec{S}_{j'} + J_3 \sum_{i''j''} \vec{S}_{i''} \cdot \vec{S}_{j''}. \quad (45)$$

determined on the square lattice shown in Fig. 5. The J_1 link is ferromagnetic and J_2, J_3 links are antiferromagnetic. For our purpose it is sufficient to consider a

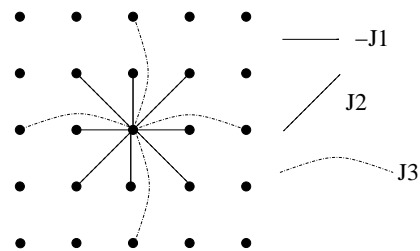


FIG. 5: 2D Heisenberg $J_1 - J_2 - J_3$ model on square lattice. There is spin \vec{S} at each site.

classical spin, $S \gg 1$. Let us impose the spiral configuration

$$\vec{S} = S(\cos(\mathbf{Q} \cdot \mathbf{r}), \sin(\mathbf{Q} \cdot \mathbf{r}), 0). \quad (46)$$

The classical energy per unit cell corresponding to the Hamiltonian (45) reads

$$E = \frac{1}{a^2} S^2 \{ -J_1 [\cos(Q_x a) + \cos(Q_y a)] + 2J_2 \cos(Q_x a) \cos(Q_y a) + J_3 [\cos(2Q_x a) + \cos(2Q_y a)] \}, \quad (47)$$

where a is the lattice spacing. Notice that in the present section we denote by indexes x and y directions in the coordinate space. Assuming that $Qa \ll 1$ and expanding the energy in powers of Q we find

$$E = -\frac{S^2}{2} Q^2 (2J_2 + 4J_3 - J_1) \quad (48)$$

$$+ \frac{S^2 J_2 a^2}{2} Q_x^2 Q_y^2 + S^2 \frac{(16J_3 + 2J_2 - J_1)a^2}{24} (Q_x^4 + Q_y^4) .$$

To have a small nonzero Q we need a small *negative* spin stiffness term. Thus, the effective energy per unit cell in terms of the ferromagnetic n-field, $\vec{n}^2 = 1$, reads

$$E(\vec{n}) = -\frac{1}{2}\rho_s(\nabla\vec{n})^2 + b_1(\partial_x\partial_y\vec{n})^2 + \frac{1}{2}b_2[(\partial_x^2\vec{n})^2 + (\partial_y^2\vec{n})^2] . \quad (49)$$

The parameters are

$$\begin{aligned} \rho_s &= S^2(2J_2 + 4J_3 - J_1) \\ b_1 &= \frac{1}{2}S^2 J_2 a^2 \\ b_2 &= \frac{1}{12}S^2(16J_3 + 2J_2 - J_1)a^2 . \end{aligned} \quad (50)$$

It is clear that the energy (49) is the most general expansion up to the fourth order derivatives. This is true for the minimal Heisenberg model (45), and this is also true for any extension of the Heisenberg model that does not include mobile fermions. Depending on relation between the parameters b_1 and b_2 the spiral is directed along a diagonal or along an axis of the square lattice. One can also tune up b_1 and b_2 in such a way that there is a directional degeneracy. The ground state energy gain due to the spin spiral is proportional to Q^4 . All in all this is *very much* different from the chiral scenario that we have considered for the “antiferromagnetic spiral”. The effective action in the present case is

$$\begin{aligned} \mathcal{L}_{Fs} &= i\frac{S}{a^2}(\eta^\dagger\dot{\eta} - \dot{\eta}^\dagger\eta) - E(\vec{n}) . \\ \vec{n} &= \eta^\dagger\vec{\sigma}\eta . \end{aligned} \quad (51)$$

This is still a gradient expansion, but the theory is qualitatively different from (7). The AF chiral theory (7) originates from the t-J model and therefore the wave vector of the spin spiral \mathbf{Q} is naturally small, it is proportional to the small doping. In the “ferromagnetic spiral” described by the action (51) the wave vector \mathbf{Q} is small only due to accidental cancellation of different contributions to the spin stiffness. The cancellation results in a very small negative stiffness.

To be specific we consider the case $b_1 < b_2$. In this case \mathbf{Q} is directed along one of the diagonals, for example

$$\mathbf{Q} = Q \left(\frac{1}{\sqrt{2}}, \frac{1}{\sqrt{2}} \right) . \quad (52)$$

Minimization of the energy (49) gives

$$Q = \sqrt{\frac{\rho_s}{b_1 + b_2}} . \quad (53)$$

B. Spin wave excitation, linear approximation

Equation of motion generated by (51) reads

$$2i\frac{S}{a^2}\dot{\eta} = \frac{\delta E}{\delta\vec{n}} \frac{\delta\vec{n}}{\delta\eta^\dagger} . \quad (54)$$

This results in the following equation for \vec{n}

$$\dot{n}_\alpha = \frac{a^2}{S}\epsilon_{\alpha\beta\gamma} \left[\hat{D}n_\beta \right] n_\gamma . \quad (55)$$

The indexes α, β, γ denote components of vector in the spin space. The differential operator in the square brackets acting on a plane wave gives a polynomial,

$$\begin{aligned} \hat{D} &= \frac{a^2}{S} [\rho_s\Delta + 2b_1\partial_x^2\partial_y^2 + b_2(\partial_x^4 + \partial_y^4)] \\ \hat{D}e^{i\mathbf{q}\cdot\mathbf{r}} &= D_{\mathbf{q}}e^{i\mathbf{q}\cdot\mathbf{r}} \\ D_{\mathbf{q}} &= \frac{a^2}{S} [-\rho_sq^2 + 2b_1q_x^2q_y^2 + b_2(q_x^4 + q_y^4)] . \end{aligned} \quad (56)$$

Looking for solution in the form

$$\vec{n} \approx (\cos(\mathbf{Q} \cdot \mathbf{r} + \varphi_{\mathbf{q}}), \sin(\mathbf{Q} \cdot \mathbf{r} + \varphi_{\mathbf{q}}), h_{\mathbf{q}}) , \quad (57)$$

and substituting this in Eq.(55) we obtain the following equations

$$\begin{aligned} \dot{\varphi}_{\mathbf{q}} &= -[D_{\mathbf{Q}} - D_{\mathbf{q}}] h_{\mathbf{q}} \\ \dot{h}_{\mathbf{q}} &= \left[D_{\mathbf{Q}} - \frac{1}{2}D_{\mathbf{q}+\mathbf{Q}} - \frac{1}{2}D_{\mathbf{q}-\mathbf{Q}} \right] \varphi_{\mathbf{q}} . \end{aligned} \quad (58)$$

The fixed-frequency solution of these equations, $\varphi_{\mathbf{q}}, h_{\mathbf{q}} \propto \exp(-i\omega_{\mathbf{q}}t)$, results in the following frequency

$$\omega_{\mathbf{q}} = \sqrt{\left[\frac{1}{2}D_{\mathbf{q}+\mathbf{Q}} + \frac{1}{2}D_{\mathbf{q}-\mathbf{Q}} - D_{\mathbf{Q}} \right] [D_{\mathbf{q}} - D_{\mathbf{Q}}]} . \quad (59)$$

It is convenient to rewrite the frequency in the following notations

$$\begin{aligned} \omega_{\mathbf{q}} &= \Omega_0 f_{\mathbf{p}} \\ f_{\mathbf{p}} &= \sqrt{X_{\mathbf{p}} Y_{\mathbf{p}}} , \end{aligned} \quad (60)$$

where p is the dimensionless momentum defined in (16).

$$\begin{aligned} \Omega_0 &= (b_1 + b_2) \frac{Q^4 a^2}{S} , \\ X_{\mathbf{p}} &= 2(p_1^2 + \alpha p_2^2) + \frac{1}{2}p^4 + 2\alpha p_1^2 p_2^2 , \\ Y_{\mathbf{p}} &= \frac{1}{2}(1 - p^2)^2 + 2\alpha p_1^2 p_2^2 , \\ \alpha &= \frac{b_2 - b_1}{b_2 + b_1} . \end{aligned} \quad (61)$$

We remind that p_1 is directed along \mathbf{Q} and p_2 is perpendicular to \mathbf{Q} . The dispersion (60) is plotted at $\alpha = 0.5$ for

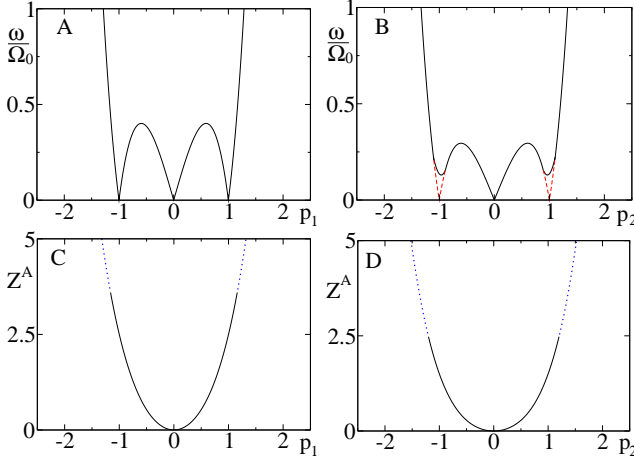


FIG. 6: (Color online) A and B: the magnon dispersion in the direction parallel to the spin spiral (A), $\mathbf{p} = (p_1, 0)$, and in the direction perpendicular to the spin spiral (B), $\mathbf{p} = (0, p_2)$. The red dashed line in Fig. B shows schematically opening of the gap driven by quantum fluctuations as it is discussed in subsection D of the present section. The “unshifted” intensity factors $Z_{\mathbf{k}}^{(A)} = \frac{\omega_{\mathbf{k}}}{\Omega_0} A_{\mathbf{k}}^2$ are plotted in Figs. (C) and (D) for the same directions. The intensity factors at values of \mathbf{k} where $\omega_{\mathbf{k}} > 0.5\Omega_0$ are shown by blue dotted lines. All the plots are presented for the anisotropy parameter $\alpha = 0.5$.

directions parallel to the spin spiral, Fig. 6A, and perpendicular to the spin spiral, Fig. 6B. There are four points to note. (i) The dispersion scales as $\Omega_0 \propto Q^4$ that is a consequence of the fourth derivatives in the action. (ii) The energy is zero at $\mathbf{p} = 0$ and at $\mathbf{p} = (\pm 1, 0)$. These zeroes are dictated by the Goldstone theorem. (iii) The energy is also zero at $\mathbf{p} = (0, \pm 1)$. These zeroes are not dictated by any exact theorem and we will see that quantum fluctuations open a gap at these points. (iv) The dispersion at $p \gg 1$ is anisotropic, $\omega_{\mathbf{q}} \approx \Omega_0 [p^4/2 + 2\alpha p_1^2 p_2^2]$. This is because the theory is stabilized by forth spacial derivatives that “know” about the lattice structure.

Representing φ and h in terms of the spin wave annihilation and creation operators ($c_{\mathbf{p}}, c_{\mathbf{p}}^\dagger$),

$$\begin{aligned} h &= \sum_{\mathbf{q}} -i A_{\mathbf{q}} c_{\mathbf{q}} e^{-i\omega_{\mathbf{q}} t + i\mathbf{q} \cdot \mathbf{r}} + h.c. \\ \varphi &= \sum_{\mathbf{q}} B_{\mathbf{q}} c_{\mathbf{q}} e^{-i\omega_{\mathbf{q}} t + i\mathbf{q} \cdot \mathbf{r}} + h.c. , \end{aligned} \quad (62)$$

and applying the standard quantization procedure to the action (51) we find the coefficients $A_{\mathbf{p}}$ and $B_{\mathbf{p}}$,

$$\begin{aligned} A_{\mathbf{p}} &= \frac{\sqrt{X_{\mathbf{p}}}}{\sqrt{2Sf_{\mathbf{p}}}} , \\ B_{\mathbf{p}} &= \frac{\sqrt{Y_{\mathbf{p}}}}{\sqrt{2Sf_{\mathbf{p}}}} . \end{aligned} \quad (63)$$

Neutron scattering amplitude is given by the Fourier transform of (57) and hence the scattering probability

with the energy transfer ω and the momentum transfer \mathbf{k} is proportional to

$$\begin{aligned} I(\omega, \mathbf{k}) &= \mathcal{R}_{\perp} A_{\mathbf{k}}^2 \delta(\omega - \omega_{\mathbf{k}}) \\ &+ \frac{1}{2} \mathcal{R}_{\parallel} \{ B_{\mathbf{k}+\mathbf{Q}}^2 \delta(\omega - \omega_{\mathbf{k}+\mathbf{Q}}) + B_{\mathbf{k}-\mathbf{Q}}^2 \delta(\omega - \omega_{\mathbf{k}-\mathbf{Q}}) \} , \end{aligned} \quad (64)$$

where \mathcal{R}_{\perp} and \mathcal{R}_{\parallel} are kinematic factors that depend on the relative orientation of the neutron polarization and the plane of the spin spiral. These factors depend on specific experimental details and therefore we do not present these factors. Thus, there is an “unshifted” contribution in the neutron scattering probability with intensity proportional to $A_{\mathbf{k}}^2$ and two “shifted” contributions with intensities proportional to $\frac{1}{2} B_{\mathbf{k} \pm \mathbf{Q}}^2$. As one expects, the intensity is diverging at points where $\omega_{\mathbf{k}} \rightarrow 0$. To characterise the intensity we plot the intensity factor $Z_{\mathbf{k}}^{(A)} = \frac{\omega_{\mathbf{k}}}{\Omega_0} A_{\mathbf{k}}^2$ in Figs. 6C and Figs. 6D for directions of \mathbf{k} parallel and perpendicular to the spiral. The “positively shifted” spectrum $\omega_{\mathbf{k}-\mathbf{Q}}$ is plotted in Fig. 7 for the direction of \mathbf{k} parallel to the spiral. In the same Fig. 7

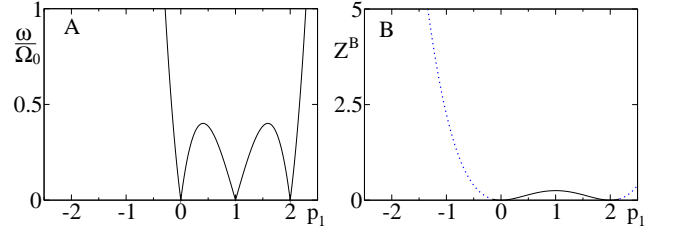


FIG. 7: (Color online) A: the positively shifted magnon dispersion $\omega_{\mathbf{k}-\mathbf{Q}}$ for the direction of \mathbf{k} parallel to the spiral. B: the intensity factor $Z_{\mathbf{k}}^{(B)} = \frac{\omega_{\mathbf{k}-\mathbf{Q}}}{2\Omega_0} B_{\mathbf{k}-\mathbf{Q}}^2$ for the positively shifted line. The intensity factor at values of \mathbf{k} where $\omega_{\mathbf{k}-\mathbf{Q}} > 0.5\Omega_0$ is shown by blue dotted line. The plots are presented for the anisotropy parameter $\alpha = 0.5$.

we also plot the intensity factor $Z_{\mathbf{k}}^B = \frac{\omega_{\mathbf{k}-\mathbf{Q}}}{2\Omega_0} B_{\mathbf{k}-\mathbf{Q}}^2$ for the shifted line. Comparing Figs. 6 C,D and Fig. 7B we conclude that the unshifted “line” has a significant amplification compared to the shifted one.

C. Quantum and thermal fluctuations. Dependence of the spiral wave vector on temperature

Since we are interested in nonlinear corrections, Eq. (57) has to be written more accurately,

$$\begin{aligned} \vec{n} &= (C_{\varphi}, S_{\varphi}, 0) \cos \gamma + (0, 0, 1) \sin \gamma \\ C_{\varphi} &= \cos(\mathbf{Q} \cdot \mathbf{r} + \varphi) \\ S_{\varphi} &= \sin(\mathbf{Q} \cdot \mathbf{r} + \varphi) \\ h &= \sin \gamma . \end{aligned} \quad (65)$$

Equations (52) and (53) have been derived by minimization of the semiclassical energy. Alternatively they can

be obtained from the condition that the linear in operators term in the action (energy),

$$\begin{aligned} E_1 = & -\rho_s (Q_x \partial_x \varphi + Q_y \partial_y \varphi) \\ & + 2b_1 Q_x Q_y (Q_y \partial_x \varphi + Q_x \partial_y \varphi) \\ & + 2b_2 (Q_x^3 \partial_x \varphi + Q_y^3 \partial_y \varphi) , \end{aligned} \quad (66)$$

is zero, $E_1 = 0$. Using (65) and expanding Eq. (49) up to cubic terms in perturbations h and φ we find the following cubic terms

$$\begin{aligned} (\nabla \vec{n})^2 & \rightarrow -2h^2 (\mathbf{Q} \cdot \nabla) \varphi \\ (\partial_\mu \partial_\nu \vec{n})^2 & \rightarrow 2 (Q_\mu \partial_\nu \varphi + Q_\nu \partial_\mu \varphi) [(\partial_\mu \varphi)(\partial_\nu \varphi) \\ & - Q_\mu Q_\nu h^2 + 2\partial_\mu (h \partial_\nu h)] . \end{aligned} \quad (67)$$

There is no summation over μ and ν in (67), so one can set $\mu = x, \nu = y$ or $\mu = x, \nu = x$, etc. To calculate the tadpole, Fig. 4, with interaction (49), (67) we note that the following expectation values are nonzero

$$\begin{aligned} \mathcal{M} &= \langle (\partial_x \varphi)(\partial_x \varphi) \rangle = \langle (\partial_y \varphi)(\partial_y \varphi) \rangle \\ &= a^2 \int \frac{d^2 q}{(2\pi)^2} B_{\mathbf{p}}^2 (q_1^2 + q_2^2) \left(n_{\mathbf{q}} + \frac{1}{2} \right) \\ \mathcal{N} &= \langle (\partial_x \varphi)(\partial_y \varphi) \rangle \\ &= a^2 \int \frac{d^2 q}{(2\pi)^2} B_{\mathbf{p}}^2 (q_1^2 - q_2^2) \left(n_{\mathbf{q}} + \frac{1}{2} \right) , \\ \langle h^2 \rangle &= \int \frac{d^2 q}{(2\pi)^2} 2A_{\mathbf{p}}^2 \left(n_{\mathbf{q}} + \frac{1}{2} \right) . \end{aligned} \quad (68)$$

Here

$$n_{\mathbf{q}} = \frac{1}{e^{\omega_{\mathbf{q}}/T} - 1} \quad (69)$$

is the usual Bose distribution. We remind also that the dimensionless p is related to q by Eq.(16), and note that $\langle \partial_\mu (n_z \partial_\nu n_z) \rangle = 0$.

When calculating the tadpole the Hartree-Fock decoupling in Eqs.(49) and (67) gives two kind of terms. Terms of the first kind proportional to $\langle n_z^2 \rangle$ lead to the following renormalization

$$\begin{aligned} \rho_s &\rightarrow \rho_s (1 - \langle n_z^2 \rangle) \\ b_1 &\rightarrow b_1 (1 - \langle n_z^2 \rangle) \\ b_2 &\rightarrow b_2 (1 - \langle n_z^2 \rangle) . \end{aligned} \quad (70)$$

Obviously, this renormalization does not change Q given by Eq.(53). Terms of the second kind are proportional to \mathcal{M} and \mathcal{N} defined in (68). They generate the following fluctuation correction (tadpole) to the effective energy

$$\begin{aligned} E_3 = & 2\mathcal{M}(b_1 + 3b_2)(Q_x \partial_x \varphi + Q_y \partial_y \varphi) \\ & + 4\mathcal{N}b_1(Q_x \partial_y \varphi + Q_y \partial_x \varphi) . \end{aligned} \quad (71)$$

The renormalized spiral wave vector Q has to be found from the condition $E_1 + E_3 = 0$, see Eqs. (66), (71). This

gives the following correction to Q

$$\begin{aligned} \frac{\delta Q}{Q} &= -\frac{1}{Q^2} \sum_{\mathbf{q}} B_{\mathbf{q}}^2 [3q_1^2 + (1 + 2\alpha)q_2^2] \left(n_{\mathbf{q}} + \frac{1}{2} \right) \\ &= -\frac{Q^2 a^2}{2S} \int \frac{d^2 p}{(2\pi)^2} \sqrt{\frac{Y_{\mathbf{p}}}{X_{\mathbf{p}}}} [3p_1^2 + (1 + 2\alpha)p_2^2] \left(n_{\mathbf{p}} + \frac{1}{2} \right) \end{aligned} \quad (72)$$

We remind again that the momentum p in this equation is dimensionless, $p = q/Q$. The quantum fluctuation part of δQ , that comes from $1/2$ in $(n_{\mathbf{p}} + 1/2)$, is ultraviolet divergent as p^4 (in 3D it would be p^5). Therefore it must be renormalized to zero. The temperature dependence of Q is given by the $n_{\mathbf{p}}$ -term that is left after the renormalization.

To understand better the quantum renormalization procedure we rewrite (66) and (71) having in mind that $Q_x = Q_y = Q/\sqrt{2}$,

$$\begin{aligned} E_1 &= [-\rho_s Q + (a_1 + a_2)Q^3] \partial_1 \varphi \\ E_3 &= [2\mathcal{M}(a_1 + 3a_2)Q + 4\mathcal{N}a_1 Q] \partial_1 \varphi . \end{aligned} \quad (73)$$

Using (68) one can easily calculate \mathcal{M}, \mathcal{N} at $T=0$,

$$\begin{aligned} \mathcal{M} &= \frac{a^2}{2S} \left[\frac{\Lambda^4}{16\pi} + f_2 \Lambda^2 Q^2 + f_4 Q^4 \ln \left(\frac{\Lambda}{Q} \right) + f_6 Q^4 \right] \\ \mathcal{N} &= \frac{a^2}{2S} \left[g_2 \Lambda^2 Q^2 + g_4 Q^4 \ln \left(\frac{\Lambda}{Q} \right) + g_6 Q^4 \right] , \end{aligned} \quad (74)$$

where $\Lambda \sim 1/a$ is the ultraviolet cutoff and $f_2, f_4, f_6, g_2, g_4, g_6$ are some functions of the anisotropy α that can be easily calculated. Comparing (74) with (73) we see that the Λ^4 term renormalizes ρ_s and the $\Lambda^2 Q^2$ terms renormalize $(a_1 + a_2)$. The $Q^4 \ln(\frac{\Lambda}{Q})$ and Q^4 terms give contributions to the energy density of the order of $\sim \frac{J}{S}(Qa)^4 Q^2$. So, the $Q^4 \ln(\frac{\Lambda}{Q})$ and Q^4 terms in (74) have to be neglected since in (49) we keep only the terms $\sim JQ^2$ and $\sim J(Qa)^2 Q^2$ neglecting higher derivatives.

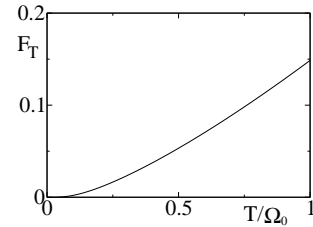


FIG. 8: Temperature dependence of the integral F_T in Eq.(75) for $Q(T)$. The value of α is 0.5

Temperature dependence of the spiral wave vector is determined by the “ $n_{\mathbf{p}}$ -part” of Eq. (72),

$$\begin{aligned} \frac{\delta Q}{Q} &= -\frac{Q^2 a^2}{2S} F_T \\ F_T &= \int \frac{d^2 p}{(2\pi)^2} \sqrt{\frac{Y_{\mathbf{p}}}{X_{\mathbf{p}}}} [3p_1^2 + (1 + 2\alpha)p_2^2] n_{\mathbf{p}} . \end{aligned} \quad (75)$$

The dimensionless integral F_T is plotted in Fig.8 versus T/Ω_0 for $\alpha = 0.5$. Temperature reduces the value of Q and this is a sizable effect.

D. Quantum correction to the spin-wave dispersion. Opening of the gap at $\mathbf{q} = (0, \pm Q)$

There is the tree leg vertex in the theory shown in Fig.9 The vertex is determined by Eqs.(49) and (67). There

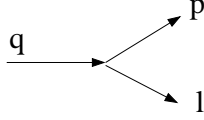


FIG. 9: The tree leg vertex

are three contributions to the vertex. The first contribution comes from the $\gamma \rightarrow \gamma\varphi$ terms shown in Fig.10 left. The second contribution comes from the $\varphi \rightarrow \gamma\gamma$ terms,

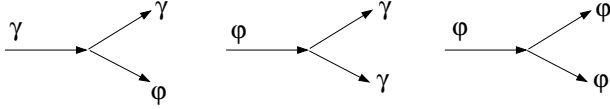


FIG. 10: Three different contributions to the 3-leg vertex

Fig.10 middle, and the third contribution comes from the $\varphi \rightarrow \varphi\varphi$ terms, Fig.10 right. A straightforward calculation gives the following answers for these contributions

$$\begin{aligned} \Gamma &= \Gamma_1 + \Gamma_2 + \Gamma_3 \\ \Gamma_1 &= 2iQ(a_1 + a_2) \times \{p_1 [p_1^2 + p_2^2(1 + 2\alpha)] A_q B_p A_l \\ &\quad + l_1 [l_1^2 + l_2^2(1 + 2\alpha)] A_q B_l A_p\} \\ \Gamma_2 &= 2iQ(a_1 + a_2) \times q_1 [q_1^2 + q_2^2(1 + 2\alpha)] B_q A_p A_l \\ \Gamma_3 &= -2iQ(a_1 + a_2) \times \{3q_1 p_1 l_1 \\ &\quad + (1 + 2\alpha) [q_1 p_2 l_2 + p_1 q_2 l_2 + l_1 p_2 q_2]\} B_q B_p B_l. \end{aligned} \quad (76)$$

Importantly, for an *on shell* scattering process, $\mathbf{q} = \mathbf{p} + \mathbf{l}$, $\omega_{\mathbf{q}} = \omega_{\mathbf{p}} + \omega_{\mathbf{l}}$, the vertex satisfies the Adler's relation, it vanishes if one of the momenta equals to 0 or \mathbf{Q} .

To understand the structure of the quantum correction to the spin-wave dispersion we calculate the $\gamma - \gamma$ polarization operator shown in Fig.11

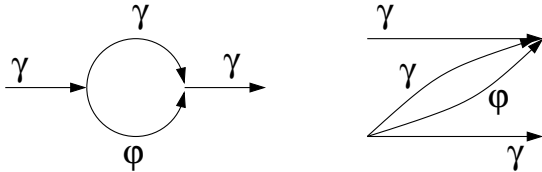


FIG. 11: The $\gamma - \gamma$ polarization operator

$$P_q^{\gamma\gamma}(\omega) = \sum_{\mathbf{k}} \frac{2\Gamma_1^* \Gamma_1(\omega_{\mathbf{q}/2-\mathbf{k}} + \omega_{\mathbf{q}/2+\mathbf{k}})}{\omega^2 - (\omega_{\mathbf{q}/2-\mathbf{k}} + \omega_{\mathbf{q}/2+\mathbf{k}})^2} \quad (77)$$

The polarization operator can be represented in the following form

$$P_q^{\gamma\gamma}(\omega) = -A_q^2 \frac{Q^2(a_1 + a_2)}{S} a^2 \times \text{integral}. \quad (78)$$

The *integral* is quadratically ultraviolet diverging. Similarly to (74) only ultraviolet diverging contributions are important with the accepted accuracy. Calculation of diverging terms in the *integral* is very simple. For example the result at $\alpha = 0.5$ is

$$\begin{aligned} \text{integral} &\rightarrow (5.2q_1^2 + 1.5q_2^2) \frac{\Lambda^2}{4\pi} + \frac{\ln(\Lambda/Q)}{2\pi} \\ &\times (8.7Q^2q_1^2 + 5.0Q^2q_2^2 - 4.7q_1^4 - 1.4q_2^4 - 10q_1^2q_2^2) \end{aligned} \quad (79)$$

The polarization operator determines the $\gamma_q^\dagger \gamma_q$ term in the effective action. The coefficient A_q^2 in (78) gives normalization of the γ -field and powers of momentum in (79) should be replaced by corresponding derivatives of this field. All in all Eq. (78) together with Eq. (79) result in the following effective energy

$$\begin{aligned} \delta E_{\gamma\gamma} &= \frac{1}{S} Q^2(a_1 + a_2) \\ &\times \left\{ - \left[5.2 \frac{(\Lambda a)^2}{4\pi} + 8.7(Qa)^2 \frac{\ln(\Lambda/Q)}{2\pi} \right] (\partial_1 \gamma)^2 \right. \\ &\quad - \left[1.5 \frac{(\Lambda a)^2}{4\pi} + 5.0(Qa)^2 \frac{\ln(\Lambda/Q)}{2\pi} \right] (\partial_2 \gamma)^2 \\ &\quad + \frac{\ln(\Lambda/Q)}{2\pi} a^2 [4.7(\partial_1^2 \gamma)^2 + 1.4(\partial_2^2 \gamma)^2 \\ &\quad \left. + 10(\partial_1 \partial_2 \gamma)^2] \right\} \end{aligned} \quad (80)$$

All momenta in the physically interesting region are of the order of Q . Hence, the typical value of the bare energy density (49) is $E_{bare} \sim \frac{S\Omega_0}{a^2}$. The logarithmic terms in (80) are of the order of $\sim \frac{\Omega_0}{a^2} (Qa)^2$, so they must be neglected within the accepted long-wave-length approximation, $Qa \ll 1$. Only the power divergent terms in (80) are significant within the long-wave-length approximation, hence

$$\delta E_{\gamma\gamma} \rightarrow - \frac{Q^2(a_1 + a_2)}{S} \frac{(\Lambda a)^2}{4\pi} [5.2(\partial_1 \gamma)^2 + 1.5(\partial_2 \gamma)^2] \quad (81)$$

The structure of $\delta E_{\varphi\varphi}$ is the same. The most important issue is that the polarization operator correction (81) contains different coefficients in front of the derivatives in different directions. To satisfy the Goldstone theorem we must introduce a contra-term $-\frac{1}{2}\delta\rho_s(\nabla\vec{n})^2$ to renormalize out the longitudinal derivative, $(\partial_1 \gamma)^2$. Because of the mentioned different coefficients the term $(\partial_2 \gamma)^2$ is not zero after the renormalization. Therefore, we necessarily open a gap in the dispersion at the points $\mathbf{q} = (0, \pm Q)$. The gap comes from fluctuations at the ultraviolet cut-off, therefore the effective field theory does not allow to calculate the gap. An estimate for the gap follows from (81),

$$\Delta \sim \frac{\Omega_0}{\pi S}. \quad (82)$$

Here we take into account that $\Lambda \sim 1/a$. The gap opening is shown schematically in Fig. 6B. Due to quantum fluctuations the gapless red dashed part of the dispersion disappears and the dispersion becomes gaped. It is worth noting that the mechanism of the gap opening due to quantum fluctuations is similar to that in the spin-stripe phase of the $J_1 - J_2$ model.^{18,19}

E. Discussion and conclusion of the “ferromagnetic spiral” section

We have formulated the effective field theory describing a spin spiral close to a collinear ferromagnetic state, i.e. the wave vector of the spiral is small compared to inverse lattice spacing, $Q \ll \pi/a$. The problem is inspired by recent data⁹ on FeSrO₃ and FeCaO₃. We assume that there are only localized spins, no mobile spin carriers. This assumption results in the effective action (51) that contains *forth* spacial derivatives. Using the effective action we calculate the spin-wave excitation spectra, see Figs.6 A,B. The spectra have three zero modes at $\mathbf{q} = 0, \pm\mathbf{Q}$ dictated by the Goldstone theorem. In the semiclassical approximation there are also two additional zero modes that are not dictated by any exact theorem. We demonstrate that quantum fluctuations open gaps at these points.

We have also calculated the temperature dependence of the spiral wave vector, $Q = Q(T)$, see Eq.(75) and Fig. 8.

The typical energy scale for the spin-wave excitation with momentum $q \sim Q$ is $\Omega_0 \propto Q^4$, see Eq.(61). The dependence $\propto Q^4$ is a consequence of the forth order derivatives in (51). Based on data⁹ we estimate that $\Omega_0 \sim 10\text{meV}$ in FeSrO₃ and FeCaO₃. Therefore an external magnetic field of the order of several Tesla can substantially modify the spin spiral making it conical.

Last but not least. The intensity of inelastic neutron scattering grows monotonously at large q , see Figs.6 B,C. Within the accepted model we do not see a way to suppress intensity outside of the region $q \sim Q$. We did calculate broadening of magnons due to the decay $1 \rightarrow 2$, see Fig. 9, and found that the broadening is very small. Introduction of mobile spins in addition to the localized ones can change the situation. In this case a redistribution of the quasiparticle weight between two brunches of the dispersion similar to that for the AF spin spiral is possible. However, discussion of this effect is outside of the scope of the present paper.

V. CONCLUSION

In the present paper we derive and analyze effective quantum field theories for helical spin magnets close to antiferromagnets and to ferromagnets. We assume that the wave vector of the spin spiral is small compared to the wave vector of the lattice, $Q \ll 2\pi/a$. The noncollinear

structure is caused by spin frustration. The field theory describing the “antiferromagnetic spin spiral” is inspired by physics of cuprate superconductors. In this case the wave vector of the spin spiral is naturally small because of the small doping x . The field theory describing the “ferromagnetic spin spiral” is inspired by the recently studied FeSrO₃ and FeCaO₃ compounds. In this case the wave vector of the spin spiral is small due to accidental fine tuning of parameters.

The effective action describing the AF spin spiral (7) contains two bosonic fields, \vec{n} corresponding to the staggered spin, and $\vec{\xi}$ corresponding to pseudospin. The action is quadratic in spacial derivatives, contains the second order time derivative of \vec{n} and the first order time derivative of the spinor field describing $\vec{\xi}$ in the CP¹ representation. The action is space and time covariant, the covariance is a consequence of the gauge invariance of the t-J model which is the origin of the effective action. The “hourglass” dispersion of magnons, see Figs. 2, 3, is a direct consequence of the action. The two branches of the “hourglass” dispersion originate from two different degrees of freedom, spin and pseudospin. The lower branch of the “hourglass” has strongly anisotropic momentum dependence with two zero modes at the Goldstone points $\mathbf{q} = \pm\mathbf{Q}$, while the upper branch is practically isotropic. This behavior agrees with the typical dispersion observed in cuprates.^{13–15} Dependent on parameters of the action the AF spin spiral can be either static or dynamic. There is a Quantum Critical Point that separates the static and the dynamic regimes. The spin spiral itself is characterised by the pseudoscalar chiral order parameter independently whether this is static or dynamic case. The chiral order parameter changes sign under time inversion.

The effective action of the ferromagnetic spin spiral, Eqs. (51) and (49), contains only one bosonic field \vec{n} describing spins. The action contains the second and the fourth order spacial derivatives as well as the first order time derivative of the spinor field describing \vec{n} in the CP¹ representation. Dependent on parameters of the action the wave vector of the spin spiral \mathbf{Q} can be directed either along a diagonal or along an axis of a square (cubic) lattice. The effective action results in the spin-wave excitation spectra shown in Figs.6 A,B. The spectra have three zero modes at $\mathbf{q} = 0, \pm\mathbf{Q}$ dictated by the Goldstone theorem. In the semiclassical approximation there are also two additional zero modes. Quantum fluctuations open gaps at these points. The wave vector of the spiral has a sizable temperature dependence that has been calculated.

Acknowledgments

We are very grateful to C. Ulrich and G. Khaliullin for communicating their results prior to publications. Discussions with them as well as with D. Efremov were very important for a significant part of this work. A. I. M.

gratefully acknowledges the School of Physics at the University of New South Wales for warm hospitality and

financial support during his visit. This work was supported in part by the Australian Research Council.

-
- * E-mail: milstein@inp.nsk.su
† E-mail: sushkov@phys.unsw.edu.au
- ¹ T. Garel and P. Pfeuty, J. Phys. C **9**, L245 (1976).
 - ² H. Kawamura, J. Appl. Phys. **63**, 3086 (1988).
 - ³ H. T. Diep, Phys. Rev. B **39**, 397 (1989).
 - ⁴ P. Azaria, B. Delamotte, and T. Jolicoeur, Phys. Rev. Lett., **64**, 3175 (1990).
 - ⁵ H. Kawamura, J. Phys.: Condens. Matter **10**, 4707 (1998).
 - ⁶ A. L. Chernyshev and M. E. Zhitomirsky, Phys. Rev. Lett., **97**, 207202 (2006).
 - ⁷ D. Belitz, T. R. Kirkpatrick, and A. Rosch, Phys. Rev. B **73**, 054431 (2006).
 - ⁸ M. Janoschek, F. Bernlochner, S. Dunsiger, C. Pfleiderer, P. Bñi, B. Roessli, P. Link, A. Rosch, arxiv: 0907.5576.
 - ⁹ C. Ulrich et al., to be published.
 - ¹⁰ B. I. Shraiman and E. D. Siggia, Phys. Rev. Lett., **61**, 467 (1988).
 - ¹¹ A. I. Milstein and O. P. Sushkov, Phys. Rev. B **78**, 014501 (2008).
 - ¹² This form of interaction with magnetic field was first pointed out by S. A. Brazovskii and I. A. Lukyanchuk, Zh. Eksp. Teor. Fiz. **96**, 2088 (1989) [Sov. Phys. JETP **69**, 1180 (1989)].
 - ¹³ J. M. Tranquada, H. Wool, T. G. Perring, H. Goka, G. D. Gu, G. Xu, M. Fujita, K. Yamada, Nature **429**, 534 (2004).
 - ¹⁴ V. Hinkov, S. Pailhes, P. Bourges, Y. Sidis, A. Ivanov, A. Kulakov, C.T. Lin, D.P. Chen, C. Bernhard, B. Keimer, Nature **430**, 650 (2004).
 - ¹⁵ V. Hinkov, P. Bourges, S. Pailhes, Y. Sidis, A. Ivanov, C. D. Frost, T. G. Perring, C. T. Lin, D. P. Chen, B. Keimer, Nature Physics **3**, 780 (2007).
 - ¹⁶ R. R. P. Singh, Phys. Rev. B **39**, 9760 (1989); Zheng Weihong, J. Oitmaa, and C. J. Hamer, Phys. Rev B **43**, 8321 (1991).
 - ¹⁷ D. Efremov and G. Khaliullin, to be published.
 - ¹⁸ R. R. P. Singh, W. Zheng, J. Oitmaa, O. P. Sushkov, and C. J. Hamer, Phys. Rev. Lett. **91**, 017201 (2003).
 - ¹⁹ G. S. Uhrig, M. Holt, J. Oitmaa, O. P. Sushkov, and R. R. P. Singh, Phys. Rev. B **79**, 092416 (2009).